Bio-Electromagnetic THz Propagation Modeling for *In-Vivo* Wireless Nanosensor Networks

Hadeel Elayan[1], Raed M. Shubair [1,2], and Josep M. Jornet [3]
[1]Department of Electrical and Computer Engineering Khalifa University, UAE
[2] Research Laboratory of Electronics, Massachusetts Institute of Technology, USA
[3] Department of Electrical Engineering, University at Buffalo, The State University of New York

***Abstract*—Nanosized devices operating inside the human body open up new prospects in the healthcare domain. In vivo wireless nanosensor networks (iWNSNs) will result in a plethora of applications ranging from intrabody health-monitoring to drug-delivery systems. With the development of miniature plasmonic signal sources, antennas and detectors, wireless communications among intrabody nanodevices will expectedly be enabled in the Terahertz Band (0.1-10 THz). This result motivates the analysis of the phenomena affecting the propagation of electromagnetic signals inside the human body. In this paper, a rigorous channel model for intrabody communication in iWNSNs is developed. The total path loss is computed by taking into account the combined effect of the spreading of the propagating wave, molecular absorption from human tissues, as well as scattering from both small and large body particles. The overall attenuation model of intrabody THz propagation facilitates the accurate design and practical deployment of iWNSNs.**

***Index Terms*—Intra-body channel modeling, nanonetworks, wireless nanosensor networks, Terahertz.**

I. Introduction

The engineering community is witnessing a new frontier in the communication industry. Among others, the tools provided by nanotechnologies enable the development of novel nanosensors and nanomachines. On the one hand, nanosensors are capable of detecting events with unprecedented accuracy. On the other hand, nanomachines are envisioned to accomplish tasks ranging from computing and data storing to sensing and actuation [1]. Recently, in vivo nanosensing systems have been presented to provide fast and accurate disease diagnosis and treatment. These systems are capable of operating inside the human body in real time and will be of great benefit for medical monitoring and medical implant communication [2].

Despite the fact that nanodevice technology has been witnessing great advancements, enabling the communication among nanomachines is still a major challenge. Classical communication paradigms need to undergo a profound revision before being used in nanonetworks. One of the mechanisms being comprehensively investigated is molecular communication [3], which is based on the exchange of molecules to transmit information. However, there are still many fundamental challenges to address, including the development of mechanisms to overcome the very long latency in molecular systems or the potential interference with biological molecular processes. Ultrasonic communication, based on the use of very high frequency acoustic signals, has also been recently proposed [4]. Nonetheless, for the time being, the size and power limitations of ultrasonic acoustic transducers pose a major challenge in their integration with biological nanosensors.

From the electromagnetic (EM) perspective, the miniaturization of a conventional metallic antenna to meet the size requirements of a nanosensor results in very high resonant frequencies, in the order of several hundreds of terahertz (THz or 10^{12} Hz). Accordingly, novel plasmonics have been recently proposed for wireless communication among nanodevices [5]. These nanoantennas enable the wireless interconnection amongst nanosensors deployed inside and over the human body resulting in many bio-nanosensing applications [6]. For the time being, several works exist pointing to both the Terahertz Band (0.1-10 THz) as well as the infrared and optical transmission windows [7] [8]. While the majority of (nano) biosensing applications rely on the use of light, the propagation of THz signals within the human body remain largely unknown.

In this paper, a novel channel model for intrabody communication in iWNSNs in the THz band is presented. In particular, a mathematical framework is developed to compute the path loss by taking into account the spreading of the propagating wave, absorption from different types of molecules, as well as scattering of both the cells and the medium background. The results provided illustrate the design principles of iWNSNs. The rest of the paper is organized as follows. In Sec. II, we discuss intrabody wave propagation losses considering the effect of spreading, molecular absorption as well as scattering. In Sec. III, the numerical results are illustrated where the absorption and scattering coefficients are calculated and the total path loss at the THz frequency is computed. Finally, we draw our conclusions in Sec. IV.

II. Intrabody Wave Propagation Losses

The total path loss in the THz band is contributed by three frequency-dependent terms: the spreading loss factor $L_{spr}(f)$, the molecular absorption loss factor $L_{abs}(f)$ and the scattering loss factor $L_{sca}(f)$. Each of these terms represents the ratio of the output to input powers for a particular intrabody distance. More specifically, the total attenuation factor is given by

$$L_{tot}(f) = L_{spr}(f) \cdot \ L_{abs}\,(f) \ \cdot L_{sca}\,(f). \qquad (1)$$

The analytical model which will be presented in this paper focuses on the frequencies between 0.1-10 THz or, equivalently, wavelengths between 30 micrometers (μm) and 3 millimeters

978-88-907018-7-0/17/$31.00 ©2017 IEEE

(mm). Moreover, since the THz band lies in the middle ground between microwaves/millimeter waves and infrared, both frequency (f) and wavelength (λ) are common notations.

A. Intrabody Path Loss Due to Wave Spreading in Human Tissue

EM waves suffer from the spreading of energy, which is quantitatively described in the case of spherical propagation by the well-known inverse-squared distance function

$$L_{spr} = D\left(\frac{\lambda_g}{4\pi d}\right)^2, \tag{2}$$

where $\lambda_g = \lambda/n'$. n is the tissue refractive index and can be written as a combination if its real, n', and imaginary parts, n'',

$$n = n' - jn''. \tag{3}$$

It is worth noting that $\epsilon_r' = n'^2 - n''^2$, where ϵ_r' is the real part of the relative permittivity, ϵ_r. We also have $n = \epsilon_r \mu_r$, where μ_r is the relative permeability. Assuming that $\mu_r = 1$, which is true for the biological tissues as they are non-magnetic, then we have $n^2 = \epsilon_r$.

The directivity, D, refers to the maximum gain of the nanoantenna, and is given by the ratio of the maximum power density $P(\theta,\phi)_{max}$ in (W/m^2) to its average value over a sphere, as observed in the far field of an antenna. Thus,

$$D = \frac{P(\theta,\phi)_{max}}{P(\theta,\phi)_{av}}. \tag{4}$$

From [9], the final form of the directivity is given by

$$D = \frac{4\pi}{\iint_{4\pi} P_n(\theta,\phi)d\Omega} = \frac{4\pi}{\Omega_A}, \tag{5}$$

where $P_n(\theta,\phi)d\Omega = P(\theta,\phi)/P(\theta,\phi)_{max}$ is the normalized power pattern, and Ω_A refers to the radiation solid angle. This angle depends on the specific radiation diagram of the source and antenna being used. For example, for a directional source with a narrow beam of width $\Delta\theta$, Ω_A is given as

$$\Omega_A = \int_{\phi=0}^{2\pi}\int_{\theta=0}^{\Delta\theta} \mathbf{sin}\theta d\theta d\phi = 2\pi(1-\mathbf{cos}\Delta\theta). \tag{6}$$

A more realistic approach would be to consider a light source with a Gaussian beam which has a radiation pattern given by [10]

$$E_\theta = \frac{1+\mathbf{cos}\theta}{2}. \tag{7}$$

Since the radiated power, P, is proportional to ${E_\theta}^2$, the solid angle, Ω_A, of a Gaussian beam of width $\Delta\theta$ is given as

$$\begin{aligned}\Omega_A &= \int_{\phi=0}^{2\pi}\int_{\theta=0}^{\Delta\theta}\frac{1}{4}(1+2\mathbf{cos}\theta+\mathbf{cos}^2\theta)\mathbf{sin}\theta d\theta d\phi \\ &= \frac{\pi}{2}\left[\frac{8}{3} - (\mathbf{cos}\Delta\theta + \mathbf{cos}^2\Delta\theta + \frac{1}{3}\mathbf{cos}^3\Delta\theta)\right].\end{aligned} \tag{8}$$

B. Intrabody Path Loss Due to Molecular Absorption by Human Tissue

Molecules present in a standard medium are excited by electromagnetic waves at specific frequencies within the THz band. An excited molecule internally vibrates, in which the atoms show periodic motion, while the molecule as a whole has constant translational and rotational motions. It must be noted that the THz waves are non-ionizing in which they induce vibration, but cannot break molecules. Due to this vibration, part of the energy of the propagating wave is converted into kinetic energy or, from the communication perspective, simply lost. Hence, molecular absorption is calculated by computing the fraction of the incident electromagnetic radiation that is able to pass through the medium at a given frequency. Using the Beer-Lambert law [11], attenuation due to molecular absorption for an EM traveling wave at a distance, d, is given by

$$L_{abs} = e^{-\mu_{abs}d}, \tag{9}$$

where μ_{abs} is the attenuation coefficient due to absorption. This coefficient depends on the composition of the medium and was first introduced and computed for gas molecules by Jornet et al in [12]. In the context of intrabody communications, the same approach is followed since the body is composed of nanoscale biomolecular structures. These include chromophores, which are compounds in our tissues responsible for absorbing light radiation. Each molecule has a spectrum of absorption that can quickly change even for small wavelength variations. The disruption of the medium optical uniformity can be expressed in the non-uniformity of the refractive index throughout the medium [13]. Hence, the attenuation coefficient due to molecular absorption can be calculated using

$$\mu_{abs} = \frac{4\pi(n'')}{\lambda}, \tag{10}$$

The imaginary term contributes to absorption; it vanishes for nonconducting particles ($\sigma = 0$) [14].

To estimate the absorption coefficient, we can follow two different strategies. On the one hand, we can model the absorption from individual particles. The efficiency of a particle to absorb radiation can be expressed by the absorption efficiency

$$Q_{abs} = \sigma_{abs}/\sigma_g, \tag{11}$$

where σ_{abs} is the molecular absorption cross section, and $\sigma_g = \pi r^2$ is the geometric cross section. Alternatively, molecular absorption can be evaluated from the absorption cross section, σ_{abs}, and the particle concentration, ρ_v, as

$$\mu_{abs} = \rho_v Q_{abs}\sigma_g, \tag{12}$$

where $\rho_v = \kappa/(\frac{4}{3}\pi r^3)$, and κ is the volume fraction of the particle. At this stage, the main challenge is to estimate the value of Q_{abs}. This is a rather complex task, specially when different types of molecules with different frequency responses are considered.

On the other hand, provided that we are dealing with a large number of molecules, it is common to consider the effective medium assumption. In particular, the dielectric response in

the frequency domain of tissues having high water content can be characterized by the Debye Relaxation Model [15], which describes the reorientation of molecules that could involve translational and rotational diffusion, hydrogen bond arrangement, and structural rearrangement. For a pure material, multiple Debye processes are possible where the complex permittivity is described by [16]

$$\epsilon(w) = \epsilon_\infty + \sum_{j=1}^{n} \frac{\Delta\epsilon}{1 + jw\tau_j}, \tag{13}$$

in which ϵ_∞ is the permittivity at the high frequency limit, $\Delta\epsilon = \epsilon_j - \epsilon_{j+1}$, ϵ_j are intermediate values, occurring at different times of the permittivity, τ_j is the relaxation time relating to the j^{th} Debye type relaxation process, and w is the angular frequency given as $2\pi f$. The disordered nature and microstructure of biological matter as well as the supracellular organization in such materials, often taking the form of fractal structures, trigger different polarization mechanisms which include multiple relaxation times and non-symmetric time-domain response.

To provide the best approximation of complex permittivity for polar liquids at frequencies up to 1 THz, the double Debye equations are used [17]

$$\epsilon(w) = \epsilon_\infty + \frac{\epsilon_1 - \epsilon_2}{1 + jw\tau_1} + \frac{\epsilon_2 - \epsilon_\infty}{1 + jw\tau_2}. \tag{14}$$

Equation (14) is rationalized and the real and imaginary parts of the complex permittivity are separated as follows

$$\epsilon'(w) = \epsilon_\infty + \frac{\epsilon_1 - \epsilon_2}{1 + (w\tau_1)^2} + \frac{\epsilon_2 - \epsilon_\infty}{1 + (w\tau_2)^2}, \tag{15}$$

$$\epsilon''(w) = \frac{(\epsilon_1 - \epsilon_2)(w\tau_1)}{1 + (w\tau_1)^2} + \frac{(\epsilon_2 - \epsilon_\infty)(w\tau_2)}{1 + (w\tau_2)^2}. \tag{16}$$

Using the values in Table I, $\epsilon'(w)$ and $\epsilon''(w)$ are computed. These values are then used to calculate (10) in order to find the attenuation due to molecular absorption, L_{abs}, given in (9).

TABLE I
PERMITTIVITY AND RELAXATION TIME VALUES

Model	ϵ_∞	ϵ_1	ϵ_2	τ_1(ps)	τ_2(ps)
Water [15]	3.3	78.8	4.5	8.4	0.1
Whole Blood [18]	2.1	130	3.8	14.4	0.1
Skin [15]	3.0	60.0	3.6	10.6	0.2

C. Intrabody Path Loss Due to Scattering by Human Tissue

From the nanosensor perspective, the body is a collection of different types of composites, such as cells, organelles, proteins, and molecules with different geometry and arrangement as well as different electromagnetic properties. Scattering by particles affect the propagation of the electromagnetic wave due to the deflection of the beam caused by the microscopic non-uniformities present in the human body. This propagation phenomenon depends on the size, shape, and refractive index of the individual particle as well as on the wavelength of the incident beam [19]. Rayleigh and Mie theories describe the scattering processes on small spherical objects. When the scattering particle diameters are smaller than the wavelength of the propagating electromagnetic wave, Rayleigh scattering occurs. On the other hand, when the particle diameters are approximately equal to the wavelength of the electromagnetic wave, Mie scattering takes place [20]. When the objects are large compared to wavelength, specular, or geometric scattering occurs [21].

The most important characteristic of a scattered wave is its intensity, I_{sca}, expressed as [14]

$$I_{sca} = \frac{1}{(kr)^2} I_{inc} F(\theta, \phi, \lambda), \tag{17}$$

where $k = 2\pi/\lambda$ is the wave number of the incident radiation, I_{inc} is the incident intensity, and $F(\theta, \phi, \lambda)$ is the scattering function. In general, $F(\theta, \phi, \lambda)$ depends on the wavelength of the incident beam and on the size, shape, and optical properties of the particle [14]. The scattering function may be represented in different forms and can be determined from theory for certain important special cases. More compactly, scattering functions have been represented in terms of basis functions such as spherical harmonics, wavelets and Zernike polynomials [22].

In addition to the intensity function, the scattering cross section and the scattering efficiency are needed to characterize the scattering loss. The scattering cross section, σ_{sca}, is defined as the ratio between the power scattered by the particle and the incident power per unit area, and is given by

$$\sigma_{sca} = \frac{1}{(k)^2} \int_0^{2\pi} \int_0^{\pi} F(\theta, \phi, \lambda) \mathbf{sin}\theta d\theta d\phi. \tag{18}$$

Analogous to absorption, the scattering efficiency, Q_{sca}, represents the ratio of the energy scattered by the particle to the total energy in the incident beam intercepted by the geometric cross section of the particle and is given by

$$Q_{sca} = \sigma_{sca}/\sigma_g. \tag{19}$$

These values depend largely on the size of the particles. In our model, we consider the scattering from both small molecules as well as relatively large cells.

1) Scattering by Particles: For particles much smaller than the wavelength, the local electric field produced by the wave is approximately uniform at any instant. This applied electric field induces a dipole in the particle. Because the electric field oscillates, the induced dipole oscillates; and according to classical theory, the dipole radiates in all directions. This type of scattering is called *Rayleigh scattering* [23].

The scattering efficiency of small spherical absorbing particles is given by [24]

$$Q_{sca}^{small} = \frac{8}{3} \psi^4 \mathbf{Re}\left(\frac{n^2 - 1}{n^2 + 2}\right)^2, \tag{20}$$

where $\psi = 2\pi r/\lambda_g$ is the dimensionless size parameter of the particle. Following a similar approach as before, we can now obtain the scattering coefficient for small particles as

$$\mu_{sca}^{small} = \rho_v Q_{sca}^{small} \sigma_g. \tag{21}$$

2) Scattering by Cells: Scattering by large particles can be studied by applying van de Hulst approximation, which is also referred to as the anomalous diffraction approximation [24]. Indeed, the total energy removed from the incident beam, the extinction energy, is the sum of the energy scattered and absorbed. The corresponding extinction efficiency is given by [25]

$$Q_{ext} = 2 - \frac{4}{p}\mathbf{sin}p + \frac{4}{p^2}(1 - \mathbf{cos}p), \tag{22}$$

in which

$$Q_{sca}^{large} = Q_{ext} - Q_{abs}, \tag{23}$$

where $p = 4\pi r(n-1)/\lambda = 2(n-1)\psi$ represents the phase delay of the wave passing through the center of the particle. The complete derivation of (22) can be found in [25]. A good example where scattering from various components can be illustrated is within the human blood. As conceptually illustrated in Fig. 1, the blood is composed of various components. Blood plasma is the liquid component of the blood and is a mixture of mostly water (up to 95% by volume) and tiny particles of dissolved protein, glucose, minerals, and so forth. It also holds different types of blood cells in suspension, which are considered as the larger particles of the blood, namely, platelets (2 microns in diameter), red blood cells (7 microns), and white blood cell (up to 20 microns).

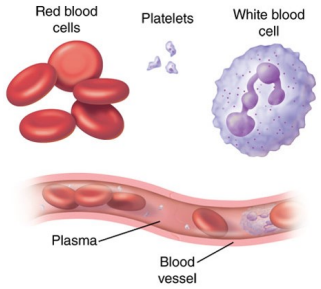

Fig. 1. Blood Components

Combining (23) and (22) in (21), we can now obtain the scattering by large particles as

$$\mu_{sca}^{large} = \rho_v Q_{sca}^{large} \sigma_g. \tag{24}$$

Finally, attenuation due to scattering is obtained from the addition of the scattering coefficient for both large and small particles, and is given as

$$L_{sca} = e^{-(\mu_{sca}^{small} + \mu_{sca}^{large})d}, \tag{25}$$

where d is the propagation distance.

III. Numerical Results

In this section, we numerically evaluate the analytical models for spreading, absorption and scattering presented in Sec. II, by taking into account realistic parameters of the intra-body properties (summarized in Table I). In this first work, we conduct our analysis for the main body constituents where we consider water, blood as well as skin.

Fig. 2 illustrates the variation of the attenuation coefficient, μ_{abs}, due to molecular absorption in terms of wavelength, for different human tissues at THz frequency. The effect of molecular absorption is more dominant in blood compared to other types of human tissues. The reason behind the high absorption in the THz is the fact that the rotation transition of water molecules is located in this band.

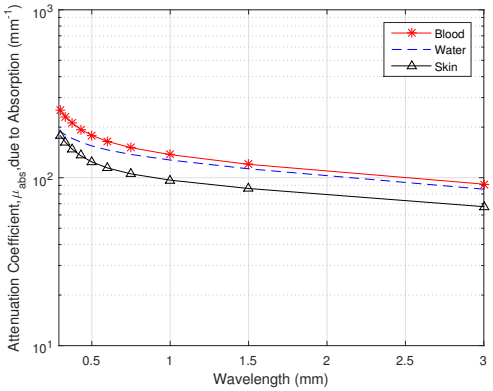

Fig. 2. Attenuation coefficient due to molecular absorption, μ_{abs}, for different human tissues vs. wavelength at THz (λ=300 μm to 3 mm).

TABLE II
Radii of Various Body Particles [26]

Body Components	Radius (m)
Water Particle	1.4×10^{-10}
Skin Cell	30×10^{-6}
Red Blood Cell	4×10^{-6}

As for the effect of scattering, (21) and (24) can be used taking into consideration the radii of the various body particles as given by Table II. It should be noted that the size of the scatterers at THz is much smaller than the wavelength of the propagating THz wave. Results of the attenuation coefficient due to scattering, μ_{sca}, given in Fig. 3 is almost negligible compared to its counterpart, absorption, given in Fig. 2.

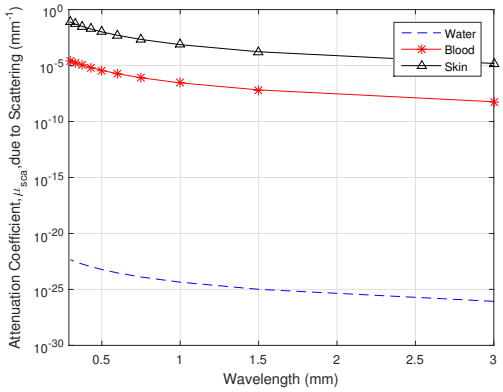

Fig. 3. Attenuation coefficient due to scattering, μ_{sca}, for different human tissues vs. wavelength at the THz frequency (λ=300 μm to 3 mm).

This finding makes sense because the scattering effect is only significant for wavelengths that are much smaller than scatterer dimensions, unlike the current case in which we are investigating scattering at the THz wavelengths. This adds to the advantages of incorporating the THz band for intrabody communication because the propagating signal will not suffer from the scattering effects which more significant in the higher optical frequencies. Based on the above finding, only the spreading and absorption losses contribute to the total path loss at THz frequencies.

The total pathloss between two nanodevices is presented in Fig. 4 for a short range communication scenario.

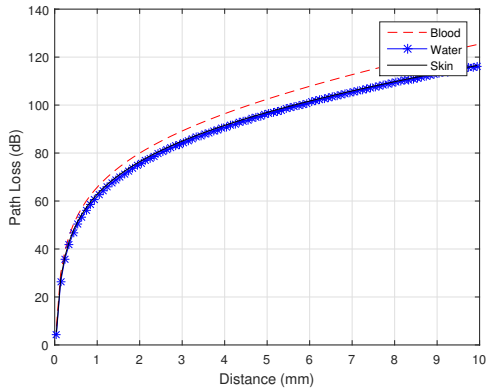

Fig. 4. Total path loss factor, L_{tot}, at (λ =300 μm), when short range communication between (0.04 mm to 10 mm) is considered.

IV. Conclusion

This paper developed a channel model for predicting the effect of THz bio-electromagnetic propagation. The presented model is novel since it takes into account the combined effect of three main propagation phenomena encountered in intrabody communication including spreading, molecular absorption, and scattering. The spreading effect has been accurately quantified by incorporating the directivity of the nanoantenna. Investigation of molecular absorption demonstrated that blood molecules are more absorbent in comparison to other body composites. Moreover, scattering has been accurately computed by taking into account the size of the scatterer nanoparticles with respect to wavelength in the THz band. The combined effects of the three main propagation phenomena in intrabody communication facilitate the design and deployment of iWNSNs. It must be highlighted that due to recent advancements in THz technologies, novel THz transmitters and receivers have been developed facilitating the communication between nanodevices and opening the door to potentially biocompatible applications of iWNSNs.

References

[1] I. F. Akyildiz, J. M. Jornet, and M. Pierobon, "Nanonetworks: A new frontier in communications," *Communications of the ACM*, vol. 54, no. 11, pp. 84–89, 2011.

[2] R. M. Shubair and H. Elayan, "In vivo wireless body communications: State-of-the-art and future directions," in *Antennas & Propagation Conference (LAPC), 2015 Loughborough*. IEEE, 2015, pp. 1–5.

[3] I. F. Akyildiz, F. Fekri, R. Sivakumar, C. R. Forest, and B. K. Hammer, "Monaco: fundamentals of molecular nano-communication networks," *IEEE Wireless Communications*, vol. 19, no. 5, pp. 12–18, 2012.

[4] G. E. Santagati, T. Melodia, L. Galluccio, and S. Palazzo, "Ultrasonic networking for e-health applications," *IEEE Wireless Communications*, vol. 20, no. 4, pp. 74–81, 2013.

[5] J. M. Jornet and I. F. Akyildiz, "Graphene-based plasmonic nano-antenna for terahertz band communication in nanonetworks," *IEEE Journal on selected areas in communications*, vol. 31, no. 12, pp. 685–694, 2013.

[6] H. Elayan, R. M. Shubair, A. Alomainy, and K. Yang, "In-vivo terahertz em channel characterization for nano-communications in wbans," in *2016 IEEE International Symposium on Antennas and Propagation (APSURSI)*, June 2016, pp. 979–980.

[7] M. Nafari and J. M. Jornet, "Metallic plasmonic nano-antenna for wireless optical communication in intra-body nanonetworks," in *Proceedings of the 10th EAI International Conference on Body Area Networks*. ICST (Institute for Computer Sciences, Social-Informatics and Telecommunications Engineering), 2015, pp. 287–293.

[8] P. Biagioni, J.-S. Huang, and B. Hecht, "Nanoantennas for visible and infrared radiation," *Reports on Progress in Physics*, vol. 75, no. 2, p. 024402, 2012.

[9] C. A. Balanis, *Antenna theory: analysis and design*. John Wiley & Sons, 2016.

[10] H. Lin, C. Fumeaux, B. M. Fischer, and D. Abbott, "Modelling of sub-wavelength thz sources as gaussian apertures," *Optics express*, vol. 18, no. 17, pp. 17 672–17 683, 2010.

[11] D. Calloway, "Beer-lambert law," *J. Chem. Educ*, vol. 74, no. 7, p. 744, 1997.

[12] J. M. Jornet and I. F. Akyildiz, "Channel modeling and capacity analysis for electromagnetic wireless nanonetworks in the terahertz band," *IEEE Transactions on Wireless Communications*, vol. 10, no. 10, pp. 3211–3221, 2011.

[13] F. Martelli, *Light Propagation Through Biological Tissue and Other Diffusive Media: Theory, Solutions, and Software*, ser. Proceedings of the Society of Photo-optical Instrumentation Engineers. SPIE Press, 2010. [Online]. Available: https://books.google.com/books?id=5pEDQgAACAAJ

[14] S. Friedlander, *Smoke, Dust, and Haze: Fundamentals of Aerosol Dynamics*, ser. Topics in chemical engineering. Oxford University Press, 2000. [Online]. Available: https://books.google.com/books?id=fNIeNvd3Ch0C

[15] K. Yaws, D. Mixon, and W. Roach, "Electromagnetic properties of tissue in the optical region," in *Biomedical Optics (BiOS) 2007*. International Society for Optics and Photonics, 2007, pp. 643 507–643 507.

[16] J. Xu, K. W. Plaxco, and S. J. Allen, "Probing the collective vibrational dynamics of a protein in liquid water by terahertz absorption spectroscopy," *protein Science*, vol. 15, no. 5, pp. 1175–1181, 2006.

[17] J. Kindt and C. Schmuttenmaer, "Far-infrared dielectric properties of polar liquids probed by femtosecond terahertz pulse spectroscopy," *The Journal of Physical Chemistry*, vol. 100, no. 24, pp. 10 373–10 379, 1996.

[18] C. B. Reid, G. Reese, A. P. Gibson, and V. P. Wallace, "Terahertz time-domain spectroscopy of human blood," *IEEE journal of biomedical and health informatics*, vol. 17, no. 4, pp. 774–778, 2013.

[19] B. Chu, *Laser light scattering*. Elsevier, 1974.

[20] J. G. Calvert, "Glossary of atmospheric chemistry terms (recommendations 1990)," *Pure and applied chemistry*, vol. 62, no. 11, pp. 2167–2219, 1990.

[21] J. A. Fozard, "Diffraction and scattering of high frequency waves," Ph.D. dissertation, University of Oxford, 2005.

[22] Y. Dong, S. Lin, and B. Guo, *Material appearance modeling: A data-coherent approach*. Springer, 2013, vol. 3.

[23] D. Bates, "Rayleigh scattering by air," *Planetary and Space Science*, vol. 32, no. 6, pp. 785–790, 1984.

[24] H. C. Hulst and H. C. van de Hulst, *Light scattering by small particles*. Courier Corporation, 1957.

[25] A. A. Kokhanovsky, *Light scattering media optics*. Springer Science & Business Media, 2004.

[26] H. P. Erickson, "Size and shape of protein molecules at the nanometer level determined by sedimentation, gel filtration, and electron microscopy," *Biological procedures online*, vol. 11, no. 1, p. 32, 2009.